# JOURNAL
OF THE
AMERICAN CHEMICAL SOCIETY

Spectroscopy of CH_3CO^- and CH_3CO

**Mark R. Nimlos,[†,‡] J. A. Soderquist,[§] and G. Barney Ellison*[,†]**

Contribution from the Department of Chemistry and Biochemistry, University of Colorado, Boulder, Colorado 80309-0215, and Department of Chemistry, University of Puerto Rico, Rio Piedras, Puerto Rico 00931. Received December 15, 1988

Abstract: We have measured the photoelectron spectra of CH_3CO^- and CH_2DCO^- and find the following electron affinities: $EA(CH_3CO) = 0.423 \pm 0.037$ eV and $EA(CH_2DCO) = 0.418 \pm 0.038$ eV. The spectra show excitation in the C–C–O bending vibration of the radical, and we have measured the following bending frequencies: $\nu_{11}(CH_3CO) = 490 \pm 30$ cm^{-1}, $\nu_{11}(CH_2DCO) = 500 \pm 50$ cm^{-1}, and $\nu_{11}(CH_3CO^-) = 570 \pm 180$ cm^{-1}. From a Franck–Condon analysis of the vibronic peak intensities we have estimated these C–C–O bond angles for the acetyl anion and radical: $\alpha(CCO)[CH_3CO^-] = 110 \pm 5°$ and $\alpha(CCO)[CH_3CO] = 133 \pm 5°$. These angles are consistent with ab initio Hartree–Fock geometry optimizations of both the ion and radical (in a triple-ζ plus polarization basis set). Finally, the electron affinities we have measured can be used to determine the following thermodynamic parameters: $\Delta H_f°_{298}(CH_3CO) = -5.4 \pm 2.1$ kcal/mol, $\Delta H_f°_{298}(CH_3CO^-) = -14.9 \pm 2.3$ kcal/mol, $DH_{298}(CH_3-CO) = 10.6 \pm 2.2$ kcal/mol, and $DH_{298}(^-CH_3-CO) = 17.6 \pm 2.3$ kcal/mol.

The acetyl radical (CH_3CO) and anion (CH_3CO^-) have been studied in many chemical systems. The radical is believed to be an intermediate in Norrish type I photofragmentation[1] of ketones. Thus in the case of acetone,[2] high-resolution FTIR studies have detected infrared emission signals from the CO and CH_3 photofragments:

$$CH_3COCH_3 + \hbar\omega_{193} \rightarrow CH_3(\nu_2=\nu_a) + [CH_3CO]^†$$

$$[CH_3CO]^† \rightarrow CH_3(\nu_2=\nu_b) + CO^† \qquad (1)$$
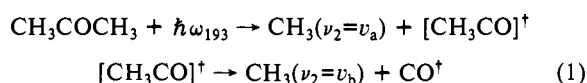
Studies of combustion chemistry have discussed the role of CH_3CO in the oxidation of hydrocarbons.[3] For example, in studies of the oxidation of vinyl radical by O atoms,[4] the acetyl radical is believed to be implicated:

$$CH_2=CH + O \rightarrow [CH_2CHO]^† \rightarrow [CH_3CO]^† \rightarrow CH_3 + CO \qquad (2)$$
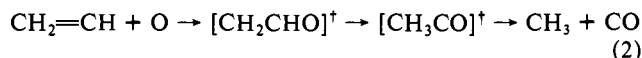
The CH_3CO radical has been formed by abstraction of hydrogen from acetaldehyde[5] with chlorine atoms. Upon reaction with NO_2 these acyl radicals produce acetoxy radicals. Acetoxy radicals are exceedingly unstable and instantly ($\cong 10^{-10}$ s^{-1}) disintegrate into methyl radicals and carbon dioxide:

$$CH_3CHO + Cl \rightarrow HCl + CH_3CO$$

$$CH_3CO + NO_2 \rightarrow NO + [CH_3CO_2]^† \rightarrow CH_3 + CO_2 \qquad (3)$$
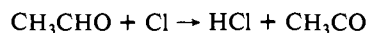
Matrix IR absorption spectra[6] of CH_3CO have been observed some time ago and report C=O stretching and methyl deformation frequencies as 1844 and 607 cm^{-1}. Studies of the electronic spectrum of acetyl find only a broad UV absorption.[7] Acyl anions have been prepared in cryogenic matrices[8] and carefully studied

---

† University of Colorado.
‡ Present address: Solar Energy Research Institute, 1617 Cole Avenue, Golden, CO 80401.
§ University of Puerto Rico.

(1) Calvert, J. G.; Pitts, J. N. *Photochemistry*; Wiley: New York, 1966. Turro, N. J. *Modern Molecular Photochemistry*; Benjamin/Cummings: Menlo Park, CA, 1978.
(2) Donaldson, D. J.; Leone, S. R. *J. Chem. Phys.* **1986**, *85*, 817. Fletcher, T. R.; Woodbridge, E.; Leone, S. R. *J. Phys. Chem.* **1988**, *92*, 5387.
(3) Warnatz, J. *Combustion Chemistry*; Springer-Verlag: New York, 1984; p 197.
(4) Heinemann, P.; Hofmann-Sievert, R.; Hoyermann, K. *Direct Study of the Reactions of Vinyl Radicals with Hydrogen and Oxygen Atoms*; Combustion Symposium, Munich, 1986.
(5) Slagle, I. R.; Gutman, D. *J. Am. Chem. Soc.* **1982**, *104*, 4741.
(6) Shirk, D. J.; Pimentel, G. C. *J. Am. Chem. Soc.* **1968**, *90*, 3349. Jacox, M. E. *Chem. Phys.* **1982**, *69*, 407.
(7) Parkes, D. A. *Chem. Phys. Lett.* **1981**, *77*, 527. Adachi, H.; Basco, N.; James, D. G. L. *Chem. Phys. Lett.* **1978**, *59*, 502.
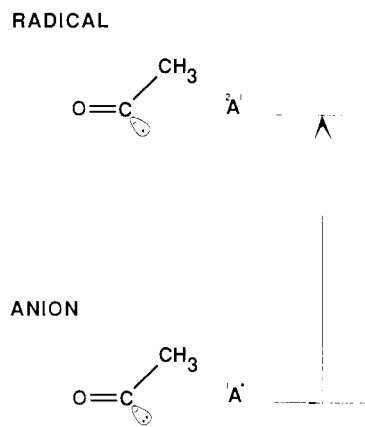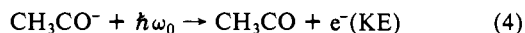
RADICAL

ANION

Figure 1. Schematic representation of the photodetachment process for the acetyl anion, CH_3CO^-. An electron is removed from the nonbonding orbital on the acyl carbon to form the acetyl radical, CH_3CO.

in a flowing afterglow device.[9]

We have investigated the photoelectron spectroscopy of the acetyl anion. To complement our experimental work, we have carried a set of ab initio, post-Hartree–Fock calculations in a large basis set.

In our photoelectron experiments, electrons are detached from mass-selected negative ions and the kinetic energy, KE, of the electrons is measured:

$$CH_3CO^- + \hbar\omega_0 \rightarrow CH_3CO + e^-(KE) \qquad (4)$$

From measurements of the kinetic energy of the scattered electrons, we can deduce the electron affinity (EA) of the resultant CH_3CO radical. Since much of the photoelectron spectrum reflects the vibrational spacings of the neutral molecule, this method can be used to study its vibrational frequencies. If transitions arising from excited anions are observed, these bands can be used to study the vibrational frequencies of the negative ion. A schematic representation of the acetyl anion and radical might anticipate the results of the process in eq 4.

To anticipate the results of our ab initio studies, consider Figure 1. This diagram suggests that the negative charge of the anion should be localized on the acyl carbon. Upon photodetachment, an electron will be removed from the doubly occupied sp^2 lobe orbital of the anion. Removing an electron from a nonbonding orbital will probably not change the bond lengths much but may affect the C–C–O bond angle. One suspects that the doubly occupied lobe orbital will interact with the rest of the electron pairs to reduce the C–C–O angle in the ion. This implies that the C–C–O angle of the radical will exceed that of the anion.

These qualitative expectations are born out by previous ab initio Hartree–Fock calculations on the anion[10] and radical.[11] In Table I we have compared the geometry of the two species as determined in these early calculations. The findings of Table I suggest that the major difference in the geometry of CH_3CO and CH_3CO^- is the C–C–O angle. One could then anticipate that the process shown in Figure 1 would result in excitation of the bending vibration of the C–C–O angle. At the bottom of Table I these is a list of the calculated harmonic frequencies of the radical. Notice that the C–C–O bend is designated as the ω_{11} mode. Although the frequencies for the radical were not assigned, it is safe to assume that the 480-cm^{-1} frequency corresponds to this bending mode. (The C–C–O bending frequency in CH_3CHO has been measured[12] and is 509 cm^{-1}.) Thus the negative ion photoelectron

Table I. Previous ab Initio Values for Acetyl Anions and Acetyl Radical

Geometry		
	CH_3CO^- (ref 10)	CH_3CO (ref 11)
$R_e(CO)$, Å	1.250	1.184
$R_e(CC)$, Å	1.574	1.513
$R_e(CH_1)$, Å	1.093	1.083
$R_e(CH_{2,3})$, Å	1.088	1.083
$\alpha(CCO)$, deg	113.1	132.2
$\alpha(CCH_1)$, deg	112.2	111.2
$\alpha(CCH_{2,3})$, deg	122.5	108.8
$\tau(OCCH_1)$, deg		0.0
$\tau(OCCH_{2,3})$, deg		±121.3

Harmonic Frequencies[11] of CH_3CO (cm^{-1})	
ω_1(C–H str) = 3285	ω_7(CH_3 def) = 1543
ω_2(C–H str) = 3284	ω_8(CH_3 rock) = 1161
ω_3(C–H str) = 3206	ω_9(C–C str) = 1085
ω_4(C–O str) = 2005	ω_{10}(CH_3 rock) = 866
ω_5(CH_3 def) = 1632	ω_{11}(C–C–O bend) = 480
ω_6(CH_3 def) = 1627	ω_{12}(torsion) = 116

spectrum will probably consist of a progression in this low-frequency vibrational mode.

The kinetic energy of the scattered electrons in eq 1 can be anticipated by employing known thermodynamic values. The EA of the CH_3CO radical can be estimated by using the $CH_3CO–H$ bond dissociation energy, DH_{298}, and the gas-phase acidity of CH_3CHO. The gas-phase acidity, ΔH_{acid}, is defined as the enthalpy of the following reaction:

$$CH_3CO–H \rightarrow [CH_3CO]^- + H^+ \qquad (5)$$

The EA can be estimated by using the following relationship:

$$EA(CH_3CO) = IP(H) + DH_{298}(CH_3CO–H) - \Delta H_{acid}(CH_3CO–H) \qquad (6)$$

A $CH_3CO–H$ bond dissociation[13–18] energy of 85 kcal/mol and a gas-phase acidity[19] of 390 ± 2 kcal/mol suggest an EA of roughly 0.3 eV. If we use the 488.0-nm (2.540 eV) line of our argon ion laser as a light source, we can expect that detached electrons will have a KE of about 2.2 eV.

Experimental Section

The apparatus used in the experiments discussed here has been described[20] in detail earlier. Briefly put, the experiment is designed so that a mass-selected anion beam crosses a fixed-frequency laser beam operating in a continuous wave mode. The two beams intersect inside the lasing cavity so that an intracavity laser power of about 75 W impinges upon the ion beam. The detached electrons are collected at right angles, and their kinetic energies are determined by a pair of double hemispherical analyzers. The analyzer voltage, V, is converted to the center-of-mass kinetic energy, KE, with the following formula:

$$KE = KE_{cal} + \gamma(V_{cal} - V) + mW\left(\frac{1}{M} - \frac{1}{M_{cal}}\right) \qquad (7)$$

where KE_{cal} ($\equiv \hbar\omega_0 - EA_{cal}$) is the kinetic energy and V_{cal} is the analyzer voltage of electrons detached from a calibration ion. Our experiments

(8) Seyferth, D.; Hui, R. C. *Organometallics* **1984**, *3*, 327.

(9) DePuy, C. H.; Bierbaum, V. M.; Damrauer, R.; Soderquist, J. A. *J. Am. Chem. Soc.* **1985**, *107*, 3385.

(10) Chandrasekhar, J.; Andrade, J. G.; Schleyer, P. R. *J. Am. Chem. Soc.* **1981**, *103*, 5612.

(11) Yadav, J. S.; Goddard, J. D. *J. Chem. Phys.* **1986**, *84*, 2682.

(12) Shimanouchi, T. *Tables of Molecular Vibrational Frequencies*; NSRDS-NBS 39, U.S. Department of Commerce, National Bureau of Standards, Washington, DC, 1972.

(13) Murad, E.; Inghram, M. G. *J. Chem. Phys.* **1964**, *41*, 404.

(14) Devore, J. A.; O'Neal, H. E. *J. Phys. Chem.* **1969**, *73*, 2644.

(15) Kerr, J. A.; Calvert, J. G. *J. Phys. Chem.* **1965**, *69*, 1022.

(16) Hole, K. J.; Mukeahy, M. F. R. *J. Phys. Chem.* **1969**, *73*, 177.

(17) Watkins, K. W.; Word, W. W. *Int. J. Chem. Kinet.* **1974**, *6*, 855.

(18) Walsh, R.; Benson, S. W. *J. Phys. Chem.* **1966**, *70*, 3751.

(19) DePuy, C. H.; Bierbaum, V. M.; Damrauer, R.; Soderquist, J. A. *J. Am. Chem. Soc.* **1985**, *107*, 3385.

(20) Ellis, H. B.; Ellison, G. B. *J. Chem. Phys.* **1983**, *78*, 6541.
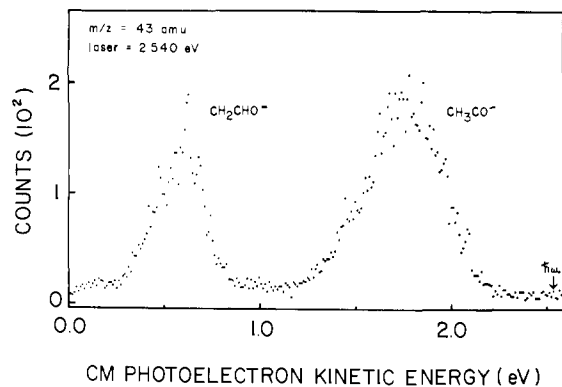
Figure 2. Fast-scan photoelectron spectrum (10 meV/point) of the ions with m/z 43. The acetaldehyde enolate ion, CH$_2$=CH—O$^-$, was positively identified from earlier photoelectron spectra.
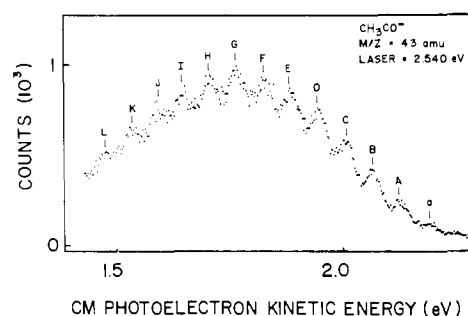

Figure 3. Slow-scan photoelectron spectrum (2.5 meV/point) of acetyl anion, CH$_3$CO$^-$. Peaks A–L correspond to a vibrational progression in the C–C–O bending vibration (ν_{11}). Peak a is a vibrational hot band.

used OH$^-$ as the calibration[21] ion; EA(OH) = 1.827 670 ± 0.000 02 eV. The kinetic energy of the ion beam was W while M and M_{cal} are the masses of the acetyl anion and the calibration ion. The compressibility factor, γ, is determined by measuring the photoelectron spectrum of Cr$^-$ and has a value of γ = 1.007 ± 0.010. We can make intense beams, 2.0–0.5 nA, of ions with a mass-to-charge ratio of 43 amu by introducing NF$_3$ and CH$_3$CO–Si(CH$_3$)$_3$ into our ion source. We feel that it is likely that in our apparatus, the acetyl anion is formed by chemistry similar to that observed in a flowing afterglow,[19,22] where the following reaction occurs:

$$F^- + (CH_3)_3Si\text{-}CO\text{-}CH_3 \rightarrow CH_3\text{-}CO^- + F\text{-}Si(CH_3)_3 \qquad (8)$$

We have also prepared a 2-nA beam of m/z = 44 amu from a mixture of NF$_3$ and the monodeuterated precursor, CH$_2$DCOSi(CH$_3$)$_3$. The deuterated silane, CH$_2$DCOSi(CH$_3$)$_3$, was synthesized by an established[23] method. Vinyl methyl ether was lithiated and treated with trimethylsilyl chloride:
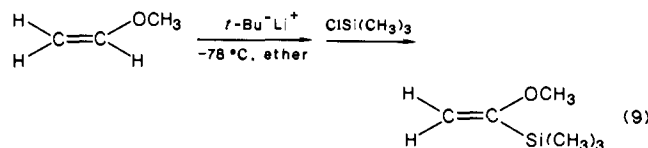
The resulting ether was hydrolyzed with a DCl/D$_2$O mixture in acetone:
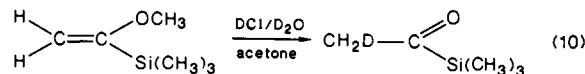
The structure of the monodeuterated product in (10) was confirmed by ^{1}H and ^{2}H nuclear magnetic resonance spectroscopy.

Results

A fast-scan (10 meV/point) photoelectron spectrum of anions with m/z 43 amu is shown in Figure 2. As expected, a feature

(21) Schulz, P. A.; Mead, R. D.; Jones, P. L.; Lineberger, W. C. *J. Chem. Phys.* **1982,** 77, 1153.

(22) DePuy, C. H.; Bierbaum, V. M.; Flippin, L. A.; Grabowski, J. J.; King, G. K.; Schmitt, R. J.; and Sullivan, S. A. *J. Am. Chem. Soc.* **1980,** 102, 5012.

(23) Soderquist, J. A.; Hsu, G. J. *Organometallics* **1982,** 1, 830.

Table II. Photoelectron Spectrum of CH$_3$CO$^-$ Laser, λ_0 = 488 nm (2.540 eV)

peak	CM KE, eV	peak interval, cm^{-1}	splitting from origin, cm^{-1}	assgnt
a	2.191 ± 0.023		570	11_1^0
A	2.120 ± 0.019	570		(0,0)
B	2.062 ± 0.019	470	470	11_0^1
C	2.001 ± 0.018	490	960	11_0^2
D	1.941 ± 0.020	480	1440	11_0^3
E	1.878 ± 0.017	510	1950	11_0^4
F	1.820 ± 0.021	470	2420	11_0^5
G	1.758 ± 0.019	500	2920	11_0^6
H	1.700 ± 0.018	470	3390	11_0^7
I	1.640 ± 0.020	480	3870	11_0^8
J	1.587 ± 0.020	430	4300	11_0^9
K	1.528 ± 0.020	480	4770	11_0^{10}
L	1.469 ± 0.017	480	5250	11_0^{11}

Table III. Photoelectron Spectrum of CH$_2$DCO$^-$ Laser, λ_0 = 488 nm (2.540 eV)

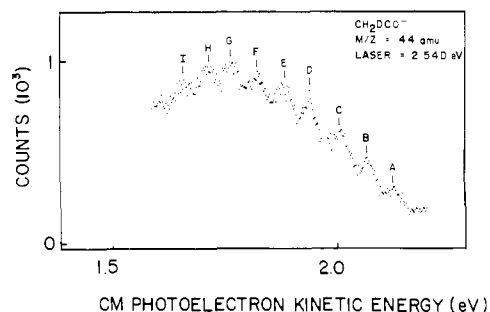| peak	CM KE, eV	peak interval, cm^{-1}	splitting from origin, cm^{-1}	assgnt
A	2.118 ± 0.021			(0,0)
B	2.061 ± 0.017	460	460	11_0^1
C	2.001 ± 0.020	490	940	11_0^2
D	1.930 ± 0.020	570	1520	11_0^3
E	1.874 ± 0.021	510	1970	11_0^4
F	1.821 ± 0.021	450	2400	11_0^5
G	1.753 ± 0.021	550	2940	11_0^6
H	1.702 ± 0.021	410	3360	11_0^7
I	1.649 ± 0.020	430	3780	11_0^8

Figure 4. Slow-scan photoelectron spectrum (2.5 meV/point) of CH$_2$D-CO$^-$. Little change is seen from the spectrum in Figure 3. Peaks A–I correspond to a vibrational progression in the C–C–O bending vibration (ν_{11}).

is observed at a KE of about 2.2 eV, and we believe this to be the acetyl anion. We are certain that the features with KE between 0 and 1 eV belong to a different ion of m/z 43 because of their intensities changed relative to the acetyl signal depending upon ion source conditions. The features of this part of the spectrum exactly match the known photoelectron spectrum[24,25] of acetaldehyde enolate, CH$_2$CHO$^-$, an isomeric ion. The observance of CH$_2$CHO$^-$ confirms our mass determination and is consistent with the chemistry of the acetyl anion. It is known that CH$_3$CO$^-$ is a strong base and that is is readily converted to the isomeric ion, CH$_2$CHO$^-$.

A slow-scan spectrum (2.5 meV/point) of the high-KE peaks is shown in Figure 3, while their positions and assignments are gathered in Table II. This spectrum shows a long progression in a low-frequency (roughly 500 cm^{-1}) vibration. The active mode in Figure 3 is approximately harmonic, and we believe that it is the C–C–O bending vibration (ω_{11}) mentioned in Table II. This is supported by examining the photoelectron spectrum of the d_1-acetyl anion, CH$_2$DCO$^-$. Since the C–C–O bending mode does

(24) Ellison, G. B.; Engelking, P. C.; Lineberger, W. C. *J. Phys. Chem.* **1982,** 86, 4873.

(25) Mead, R. D.; Lykke, K. R.; Lineberger, W. C.; Marks, J.; Brauman, J. I. *J. Chem. Phys.* **1984,** 81, 4883.

7678   *J. Am. Chem. Soc., Vol. 111, No. 20, 1989*

Nimlos et al.

not involve the motion of hydrogen, one would expect a very small shift in the peak positions upon deuteration. The slow-scan spectrum for CH_2DCO^- is displayed in Figure 4, and the peak positions shown in Table III. These results indicate that there is no change in the vibrational spacings. Attempts to prepare beams of CD_3CO^- were not successful.

Discussion

Photoelectron Assignments. The long vibrational progression in the photoelectron spectrum originates at a KE of approximately 2.2 eV and leads to an EA of about 0.3 eV. We can obtain a more precise EA by considering the high-energy features in Figure 3. By changing the ion source conditions, we have been able to change the intensity of peak **a** relative to peak **A**. This suggests that peak **a** is a hot band and that peak **A** is the origin of the spectrum. Referring to Table II and III, we extract an uncorrected or raw EA by subtracting the KE of this peak from the laser energy so that we find the raw $EA(CH_3CO) = 0.420 \pm 0.019$ eV and raw $EA(CH_2DCO) = 0.422 \pm 0.021$ eV. We must make corrections to this value below to take into account the fact that we detach from vibrationally and rotationally excited ions. We can also assign the fundamental frequency for the C–C–O bend in the radical and the anion. If we take the difference of peak **B** from peak **A**, we obtain $\nu_{11}(CH_3CO) = 470 \pm 150$ cm^{-1} and $\nu_{11}(CH_2DCO) = 460 \pm 150$ cm^{-1}. By subtracting A from **a**, we get $\nu_{11}(CH_3CO^-) = 570 \pm 180$ cm^{-1}. To extract a more accurate value for the CH_3CO frequency, we assume the Franck–Condon profile in Figure 3 is derived from a single oscillator and fit all of the peaks in our spectra to a simple power series:

$$G(v) = \omega_{11}(v + \tfrac{1}{2}) - x_{11,11}(v + \tfrac{1}{2})^2 \qquad (11)$$

The data are best fit by $\omega_{11}(CH_3CO) = 490 \pm 30$ cm^{-1}, $x_{11,11}(CH_3CO) = -1.3 \pm 3.4$ cm^{-1}, $\omega_{11}(CH_2DCO) = 500 \pm 50$ cm^{-1}, and $x_{11,11}(CH_2DCO) = -3.0 \pm 7.5$ cm^{-1}. These values suggest that the vibrational motion we observe is essentially harmonic and is insensitive to isotopic substitution.

The fact that there is little shift in the peak positions upon deuteration allows us to unambiguously assign the observed low-frequency mode as the C–C–O bend. This can be seen by considering all possible low-frequency vibrational modes listed in Table I. These modes include two CH_3 rocks (ω_8 and ω_{10}), the C–C stretch (ω_9), the CH_3 torsional motion (ω_{12}), and the C–C–O bending motion (ω_{11}). We can discount the C–C stretch in Figure 3 because the vibration we see has a low frequency and is harmonic. Typically, C–C stretches[12] have frequencies slightly over 1000 cm^{-1}, and the computations in Table I echo this generality. It might be argued that since the C–C bond in acetyl radical is very weak[13] $[DH_{298}(CH_3-CO) = 11.3 \pm 0.7$ kcal/mol], the C–C stretch could have a lower frequency than is commonly found. However, a weak C–C bond will also cause the C–C stretching to be very anharmonic. This will be especially true as the vibrational levels approach the dissociation limit. Table II shows that the mode seen remains essentially harmonic up to 15 kcal/mol above the ground state. This is very close to the dissociation limit and seems to rule out the C–C stretch. By comparison the HCO radical has a weak[26] C–H bond $[DH_{298}(H-CO) = 18 \pm 2$ kcal/mol], a C–H stretching frequency[27] of 2790 cm^{-1}, and a C–H stretching anharmonicity of 165 cm^{-1}. Since there was no observable deuterium shift in vibronic bands of the photoelectron spectrum, we can also eliminate the possibility that CH_3 rocking or torsional motions are being excited. These motions can be estimated[28] to have an effective mass proportional to $[3M_H]^{-1/2}$, which may be used to rationalize the observed deuterium shifts in CH_3CHO. If this same mass term is applied to the observed harmonic frequency for CH_3CO (490 cm^{-1}), we would expect the
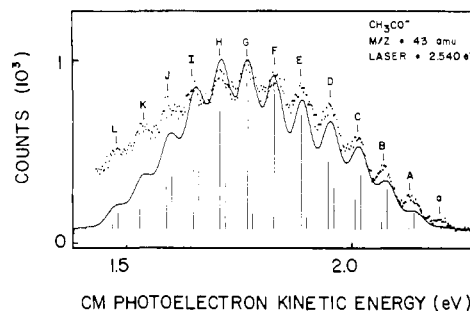

Figure 5. Results of Franck–Condon analysis. Points are experimental data and vertical lines are calculated intensities. The smoothed line is a synthesized spectrum that is obtained by folding Gaussians of an experimental width (50 meV) with these intensities.

monodeuterated species to have a frequency of 440 cm^{-1}. Since we see little shift in any of the peak positions, we have assigned the spacings as due to the C–C–O bend, ω_{11}.

We have calculated Franck–Condon factors in an attempt to model the photoelectron spectra. Franck–Condon factors were obtained by estimating reasonable potential energy curves, solving for the vibrational wave functions, and then calculating the square of the overlaps of these functions. Several drastic assumptions are made to model our spectrum. We have attempted to fit the entire profile in Figure 3 with vibronic bands involving only a single active mode, the C–C–O bend. This may be a severe restriction considering the photoelectron spectrum[27] of HCO$^-$. In the photodetachment process for the formyl anion, the C–H and C=O bond lengths changed by an amount comparable to the calculated changes for the C–C and C=O bond lengths in CH_3CO^- (Table I). The photoelectron spectrum of HCO$^-$ showed excitations in the C–H and C=O stretching frequencies of the HCO radical in addition to the bend. However, the peaks for these vibronic bands had a lower intensity than the peak corresponding to the origin. If a similar situation occurred for CH_3CO^-, the vibronic peaks for excitation in the C–C and C=O stretches might be expected to have a lower intensity than peak **A**. Features that weak would be difficult to resolve in our spectrum. We also assume that the bending mode is an uncoupled harmonic vibration and that the force constants can be determined in a routine way from the frequencies in Table II. For simplicity's sake we have conjectured that the motion could be described as a triatomic motion where the methyl group (CH_3-) bends onto a C=O group. The effective mass for this oscillator was estimated as the reciprocal of the Wilson G matrix[29] element:

$$g_{bend} = R^{-2}M_{Me}^{-1} + r^{-2}M_O^{-1} +$$
$$[R^{-2} + r^{-2} - R^{-1}r^{-1}\cos \alpha(CCO)]M_C^{-1} \qquad (12)$$

In this expression, R and r are the C–C and C–O bond lengths, $\alpha(CCO)$ is the C–C–O bond angle, and M_{Me}, M_C, and M_O are the masses of the methyl group, the carbon atom, and the oxygen atom. We used the bond distances in Table I and varied the bond angles, $\alpha(CCO)$, until the intensities matched the spectrum in Figure 3. Observed peak heights were also affected by sequence bands whose intensities were determined by Franck–Condon factors and a variable effective vibrational temperature. Since we have assumed that the bending mode is harmonic, we need only determine the difference in bond angle between the ion and the radical. We found the best fit with a change in bond angle of 23.5° and a temperature of 1200 K. The fit is shown in Figure 5 where the points are the experimental data and the vertical lines are the calculated intensities. The synthesized spectrum was obtained by folding these intensities with Gaussians of an experimental width (50 meV). We obtained a fairly good fit to the observed peak positions but seem to have trouble with some of the peak intensities. This may be a result of having ignored couplings with the C–C and C=O stretches. However our ex-

(26) Moortat, G. K.; Seiler, W.; Warnek, P. *J. Chem. Phys.* **1983**, *78*, 1185.

(27) Murray, K. K.; Miller, T. M.; Leopold, D. G.; Lineberger, W. C. *J. Chem. Phys.* **1986**, *84*, 2520.

(28) Herzberg, G. *Molecular Spectra and Molecula Structure: II. Infrared and Raman Spectra of Polyatomic Molecules*; Van Nostrand: New York, 1945.

(29) Wilson, E. B.; Decius, E. C.; Cross, P. C. *Molecular Vibrations*; McGraw-Hill: New York, 1955; Appendix VI.

Spectroscopy of CH₃CO⁻ and CH₃CO

J. Am. Chem. Soc., Vol. 111, No. 20, 1989 7679

perimentally derived change in α(CCO) agrees with the calculated value of 19.1° in Table I.

Thermochemistry. Several thermodynamic values can be determined by using the EA from this study. First, a rotational correction[30] must be made to the raw EA. This correction is due to the fact that the anions are distributed over a number of rotational states and its derivation is outlined elsewhere.[31,32] For an asymmetric top, this correction has been estimated to be

$$\Delta_{rot} = k_B T[\tfrac{1}{2} - (A'/2A'') - (B'/2B'') - (C'/2C'')] \qquad (13)$$

where the rotational constants for the anion $(A'', B'', \text{and } C'')$ and the radical $(A', B', \text{and } C')$ were determined for the geometries in Table I. We used the same temperature, T, that was needed for the Franck–Condon fit (1200 K). Corrections of -0.007 ± 0.027 eV for the d_0 anion and -0.014 ± 0.027 eV for the d_1 anion were added to the raw EAs. A sequence band correction also had to be made due to the fact that ions were vibrationally excited. This correction is discussed elsewhere.[30] Briefly, we are concerned with the fact that the anion and the radical have a different vibrational frequencies. If the vibrational temperature is high enough, the sequence bands can actually shift the origin of the spectrum by a fraction, η, of this difference; thus $\Delta_{sequence} = \eta\Delta\omega$. In this case, the constant η is close to 1 and the correction is 0.0099 $\pm$ 0.017 eV. This correction is also added to the raw EAs, giving the following adiabatic EAs: EA(CH₃CO) = 0.423 $\pm$ 0.037 eV and EA(CH₂DCO) = 0.418 $\pm$ 0.038 eV.

The heat of formation of the acetyl radical can be determined from its EA and the gas-phase acidity of acetaldehyde:

$$\Delta H_f{}^\circ{}_{298}(CH_3CO) = \Delta H_{acid}(CH_3CO-H) + EA(CH_3CO) - \Delta H_f{}^\circ{}_{298}(H+) + \Delta H_f{}^\circ{}_{298}(CH_3CHO) \qquad (14)$$

where[33] $\Delta H_f{}^\circ{}_{298}(CH_3CHO) = -39.63 \pm 0.10$ kcal/mol. We obtain a value of $\Delta H_f{}^\circ{}_{298}(CH_3CO) = -5.4 \pm 2.1$ kcal/mol. This compares well with earlier values (-5.1 ± 2.0 kcal/mol) measured[13] from the study of appearance potentials in mass spectroscopy. Use of $\Delta H_f{}^\circ{}_{298}(CH_3CO) = -5.4 \pm 2.1$ kcal/mol together with our experimental electron affinity[34] yields a value for the heat of formation of the acetyl anion, $\Delta H_f{}^\circ{}_{298}(CH_3CO^-) = -14.9 \pm 2.3$ kcal/mol.

In light of this heat of formation and gas-phase acidity, it is interesting to compare H atom migration in the acetyl radical
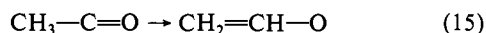
$$CH_3-C{=}O \rightarrow CH_2{=}CH-O \qquad (15)$$

to H migration in the anion
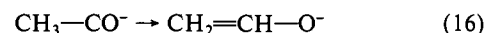
$$CH_3-CO^- \rightarrow CH_2{=}CH-O^- \qquad (16)$$

For the radical it is endothermic for CH₃CO to rearrange to CH₂CHO [$\Delta H_{rxn}(12) = +8.2 \pm 4.3$ kcal/mol], while it is exothermic[35] for the CH₃CO⁻ to isomerize to CH₂CHO⁻ [$\Delta H_{rxn}(13) = -24 \pm 3$ kcal/mol]. Presumably the enolate anion, CH₂CHO⁻, is stabilized by two resonance forms. The barriers for these rearrangements are not known and they could be expected to be high.

It is informative to contrast the acetyl (CH₃CO) and formyl systems (HCO). Both the acetyl[36] and formyl[37] radicals are bent

---

(30) Nimlos, M. R.; Ellison, G. B. *J. Am. Chem. Soc.* **1986**, *108*, 6522.

(31) Engelking, P. C. *J. Phys. Chem.* **1986**, *90*, 4544.

(32) Nimlos, M. R. Ph.D. Thesis, University of Colorado, Boulder, CO, 1986.

(33) Pedley, J. B.; Rylance, J. *Sussex-NPL Computer Analysed Thermochemical Data: Organic and Organometallic Compounds*; University of Sussex, Brighton, England, 1977.

(34) We use the convention that the heat of formation of a free electron is 0.

(35) Bartmess, J. E.; Scott, J. A.; McIver, R. T., Jr. *J. Am. Chem. Soc.* **1979**, *101*, 6047.

(36) This work.

(37) Tjossem, P. J. H.; Cool, T. A.; Webb, D. A.; Grant, E. R. *J. Chem. Phys.* **1988**, *88*, 617.

(38) Chuang, M.; Foltz, M. F.; Moore, C. B. *J. Chem. Phys.* **1987**, *87*, 3855.

Table IV. Experimental Molecular Constants

EA(CH₃CO) = 0.423 $\pm$ 0.037 eV	EA(CH₂DCO) = 0.418 $\pm$ 0.038 eV
$\Delta H_f{}^\circ{}_{298}$(CH₃CO) = -5.4 ± 2.1 kcal/mol	$\Delta H_f{}^\circ{}_{298}$(CH₃CO⁻) = -14.9 ± 2.3 kcal/mol
DH$_f{}^\circ{}_{298}$(CH₃–CO) = 10.6 ± 2.2 kcal/mol	DH$_f{}^\circ{}_{298}$(⁻CH₃–CO) = 17.6 ± 2.3 kcal/mol
ν_{11}(CH₃CO) = 490 $\pm$ 30 cm⁻¹	ν_{11}(CH₃CO⁻) = 570 $\pm$ 180 cm⁻¹
ν_{11}(CH₂DCO) = 500 $\pm$ 50 cm⁻¹	
α(CCO)[CH₃CO] = 133 $\pm$ 5°	α(CCO)[CH₃CO⁻] = 110 $\pm$ 5°

Table V. Ab Initio Calculations of the Acetyl Radical (CH₃CO)

E(UHF) = $-152.343\,174$ hartree
6-311++G** basis set
$\langle S^2 \rangle$ = 0.7617
μ_D = 2.968 D
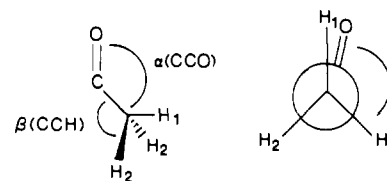
$\tilde{X}$ (²A′) acetyl radical

UHF Optimized Geometry in a 6-311++G** Basis Set

R_e(CO) = 1.157 Å, R_e(CC) = 1.510 Å, R_e(CH₂) = 1.084 Å, R_e(CH₁) = 1.085 Å
α(CCO) = 130.1°, β(CCH₂) = 108.6°, β(CCH₂) = 110.6°
τ(OCCH₂) = 121.4°, τ(OCCH₁) $\equiv$ 0°
rotational constants: A = 2.943 cm⁻¹, B = 0.334 cm⁻¹, C = 0.318 cm⁻¹
$\kappa \equiv (2B - A - C)/(A - C) = -0.987$

Vibrational Modes

mode	harmonic freq, cm⁻¹	scaled (0.89) freq, cm⁻¹	int, atm⁻¹ cm⁻²
ω_1 a′	3263	2904	48.9
ω_2 a″	3262	2903	27.3
ω_3 a′	3175	2826	29.5
ω_4 a′	2120	1886	1167.2
ω_5 a″	1579	1405	53.6
ω_6 a′	1576	1402	85.6
ω_7 a′	1489	1325	36.7
ω_8 a′	1152	1025	73.8
ω_9 a″	1039	925	0.3
ω_{10} a′	918	817	6.9
ω_{11} a′	510	454	39.0
ω_{12} a″	106	94	0.002

species: α(CH₃–CO) = 133 $\pm$ 5° and α(H–CO) = 124.95 $\pm$ 0.25° and each has low electron affinities: EA(CH₃CO) = 0.423 $\pm$ 0.037 eV while[27] EA(HCO) = 0.313 $\pm$ 0.005 eV. In both cases the ions are strongly bent with α(CH₃–CO⁻) = 113 $\pm$ 5° and α(H–CO⁻) = 109 $\pm$ 2°. Bond dissociation energies in these systems are unusually small:

reaction	DH$_f{}^\circ{}_{298}$, kcal/mol	ref
H–CO → H + CO	15.69 $\pm$ 0.19	38
CH₃–CO → CH₃ + CO	10.6 $\pm$ 2.2	this work
H–CO⁻ → H⁻ + CO	5.5 $\pm$ 0.2	27
CH₃–CO⁻ → CH₃⁻ + CO	17.6 $\pm$ 2.3	this work

Ab Initio Electronic Structure Calculations. To gain some added insight into our experimental findings, we have carried out a set of ab initio calculations on both the CH₃CO radical as well as the CH₃CO⁻ ion. We have utilized the GAUSSIAN-86 package[39] of electronic structure programs to investigate the properties of these species. Hartree–Fock calculations in a split basis set (3-21G) were initially used to survey the acetyl radical and the acetyl anion. It is well-known[40] that unrestricted Hartree–Fock wave

---

(39) Binkley, J. S.; Whiteside, R. A.; Raghavachari, K.; Seeger, R.; DeFrees, D. J.; Schlegel, H. B.; Frisch, M. J.; Pople, J. A.; Kahn, L. R. GAUSSIAN-86; Carnegie-Mellon University, Pittsburgh, PA, 1986.

Table VI. Ab Initio Calculations of the Acetyl Anion (CH_3CO^-)

E(RHF) = −152.309 946 hartree
6-311++G** basis set

$\tilde{X}$ ($^1A'$) acetyl anion
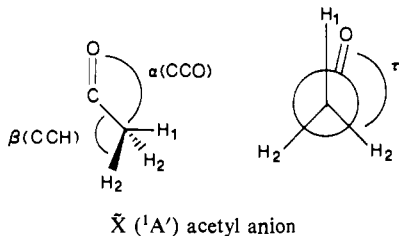
RHF Optimized Geometry in a 6-311++G** Basis Set
R_e(CO) = 1.216 Å, R_e(CC) = 1.579 Å, R_e(CH$_2$) = 1.092 Å,
R_e(CH$_1$) = 1.098 Å
α(CCO) = 113.1°, β(CCH$_2$) = 108.6°, β(CCH$_2$) = 112.4°
τ(OCCH$_2$) = 121.9°, τ(OCCH$_1$) ≡ 0°
rotational constants: A = 2.103 cm^{-1}, B = 0.355 cm^{-1},
 C = 0.321 cm^{-1}
$\kappa \equiv (2B - A - C)/(A - C) = -0.963$

Vibrational Modes

mode	harmonic freq, cm^{-1}	scaled (0.89) freq, cm^{-1}	int, atm^{-1} cm^{-1}
ω_1 a$''$	3149	2803	237.3
ω_2 a$'$	3133	2788	350.3
ω_3 a$'$	3039	2705	636.8
ω_4 a$'$	1697	1510	2575.9
ω_5 a$''$	1565	1393	36.6
ω_6 a$'$	1558	1387	117.5
ω_7 a$'$	1386	1234	536.0
ω_8 a$'$	1078	960	222.6
ω_9 a$''$	921	820	191.9
ω_{10} a$'$	781	695	311.3
ω_{11} a$'$	544	484	29.9
ω_{12} a$''$	115	102	12.6

functions for radicals are not proper eigenfunctions of S^2 and are contaminated with higher multiplets; consequently $\langle S^2 \rangle$ for the $^2A'$ radical $CH_3CO \neq {}^3/_4$. Final geometry optimizations for the CH_3CO and the CH_3CO^- species were carried out in a triple-ζ basis set augmented with polarization and diffuse functions (6-311++G**). These geometry searches are carried out by analytic calculation[41] of the energy gradients. Once the equilibrium geometry is found, the harmonic vibrational frequencies, $\{\omega\}$, can be solved for. The results of these ab initio calculations are displayed in Tables V and VI.

In the case of CH_3CO, our findings parallel the earlier Hartree–Fock findings.[11] The only noticeable difference is the contraction of the C=O bond from 1.184 Å (3-21G) to 1.157 Å (6-311++G**). Our radical is nearly a prolate top (κ = −0.987) and is quite a polar species with a calculated dipole moment, μ_D = 2.968 D. The larger basis set of Table V yields an energy, E(UHF), 0.905 hartree lower than earlier calculations: E(6-311++G**) < E(3-21G). To correct for electron correlation, we have carried out a single point, second-order Møller–Plesset calculation for the acetyl radical using the UHF geometry reported in Table V. Thus we find E(UHF)[CH_3CO] = −152.343 174 hartree while E(MP2)[CH_3CO] = −152.860 509 hartree.

If the C–C–O angle in CH_3CO is constrained to be 180°, the radical then has C_{3v} symmetry and the lowest energy configuration is a ^2E state. We can write a GVB expression[42] which relates the $\tilde{X}$ ($^2A'$) state of CH_3–CO and the first electronic state $\tilde{A}$ ($^2A''$) to the linear ^2E configuration (eq 17).
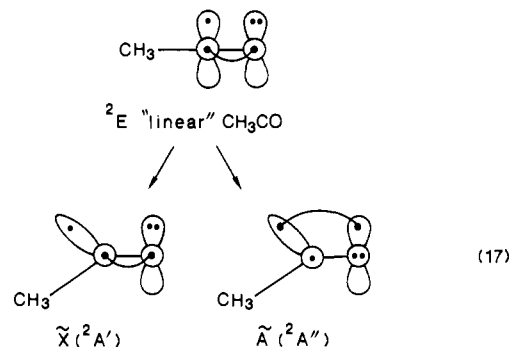
The C–C–O bending motion splits the doubly degenerate ^2E state into the ground $\tilde{X}$ A$'$ and excited $\tilde{A}$ A$''$ states shown in eq 17. If we treat this radical as a triatomic, the ground $\tilde{X}$ state has a bent configuration (Me—C=O) while the excited $\tilde{A}$ state is closer to linearity. This is similar to the Renner–Teller splitting[43] in the formyl radical, HCO. With the formyl radical, the bending motion splits the degenerate $^2\Pi$ state of linear HCO into a bent ground state, $\tilde{X}$ $^2A'$, and a linear excited state, $\tilde{A}$ $^2A''$. The energy of linear formyl radical is known to be 26.6 kcal/mol above the bent ground state. The fact that the formyl radical and the acetyl radical are bent by about the same amount (Table V) suggests that their barriers may be comparable. We have used a UHF calculation in a 6-311++G** basis to estimate the splitting between ground-state CH_3CO and the linear, ^2E state of CH_3CO. Following geometry optimization for the linear, C_{3v} acetyl radical, we compute E(UHF) = −152.294 855 hartree. Consequently our estimate of the splitting between the pair of acetyl states in (17) is ΔE(UHF) = 48.3 mhartree or about 30 kcal/mol. Thus T_e for the $\tilde{A}$ state of acetyl should be roughly 1.3 eV. However, it is difficult to identify this $\tilde{A}$ state in our experimental photoelectron spectra because of unfavorable Franck–Condon factors and interference from the spectrum of CH_2CHO^-.

The harmonic vibrational frequencies for the CH_3CO radical are very interesting. We calculate that the C–C–O bending mode, ω_{11}(a$'$) has a frequency of 510 cm^{-1}, which is scaled[44] by 0.89 to 454 cm^{-1}. We estimate the IR absorption intensity[45] of this normal mode to be roughly, S = 39.0 atm^{-1} cm^{-2}. Recall the experimental estimate of the CH_3–CO bending mode from Table IV is ν_{11}-(CH_3CO) = 490 ± 30 cm^{-1}; we use ν to refer to our experimental frequencies to contrast them with the harmonic approximations, ω. The Hartree–Fock value for the C–C–O angle, 130.1°, also compares favorably with our estimates from the Franck–Condon analysis of our spectra, which yielded a value (see Table IV) α(CCO) = 133 ± 5°.

RHF calculations in a 6-311++G** basis on the CH_3CO^- ion yield a molecular structure similar to that reported[10] earlier. Comparison of Table I with Table VI indicates that use of the 6-311++G** basis leads to a shorter C=O bond for the acetyl anion. The harmonic vibrational frequencies for the CH_3CO^- ion are listed in Table VI, and the C–C–O bending frequency ω_{11}(a$'$) has a frequency of 544 cm^{-1}, which is scaled by 0.89 to 484 cm^{-1}. The single hot band that we identify leads us to assign ν_{11}-(CH_3CO^-) = 570 ± 180 cm^{-1}, consistent with our computed frequency.

Notice that at the Hartree–Fock level of approximation the acetyl anion is not bound; that is, E(UHF)[CH_3CO] = −152.343 174 hartree while E(RHF)[CH_3CO^-] = −152.309 946 hartree, so the ion is 33.2 mhartree up in the continuum. An explicit consideration of zero-point corrections does not change this. If one now correlates the acetyl ion, matters improve. A MP2 calculation of the CH_3CO^- ion at the RHF minimum (listed in Table VI) leads to a significant lowering of the anion's energy:

(40) Szabo, A.; Ostlund, N. S. *Modern Quantum Chemistry: Introduction to Advanced Electronic Structure Theory*; Macmillan: New York, 1982.

(41) Pulay, P. In *Applications of Electronic Structure Theory*, Schaefer, H. F., III, Ed.; Plenum Press: New York, 1977; Chapter 4, pp 153–186.

(42) Goddard, W. A.; Harding, L. B. *Annu. Rev. Phys. Chem.* **1978**, *29*, 363.

(43) Tjossem, P. J. H.; Cool, T. A.; Webb, D. A.; Grant, E. R. *J. Chem. Phys.* **1988**, *88*, 617.

(44) Hess, B. A., Jr.; Schaad, L. J.; Cársky, P.; Zahradník, R. *Chem. Rev.* **1986**, *86*, 709.

(45) Pugh, L. A.; Rao, K. N. In *Molecular Spectroscopy: Modern Research II*; Academic Press: New York, 1976; Chapter 4, p 165.

E(MP2)[CH$_3$CO$^-$] = −152.864142 hartree. As mentioned above, E(MP2)[CH$_3$CO] = −152.860509 hartree so the acetyl ion is now predicted to be bound, with respect to CH$_3$CO and a free electron, by 3.6 mhartree or 0.1 eV. Instead of subtracting the total energies of the anion and radical, one might use Koopmans' approximation[40] to estimate the electron affinity. Use of the highest occupied orbital for CH$_3$CO$^-$, ψ_{12}(a′) with eigenvalue ϵ_{12} = −0.0448, leads to a "frozen orbital" EA ≅ 1.2 eV. These theoretical estimates should be compared with our experimental finding of EA(CH$_3$CO) = 0.423 ± 0.037 eV.

Conclusions

The results of our experimental findings are summarized in Table IV and Figure 5. Our ab initio calculations are collected together in Tables V and VI and are entirely congruent with our experimental results.

SERRS of Langmuir–Blodgett Monolayers: Spatial Spectroscopic Tuning

Ricardo Aroca* and U. Guhathakurta-Ghosh

Contribution from the Department of Chemistry & Biochemistry, University of Windsor, Windsor, Canada N9B 3P4. Received February 7, 1989

Abstract: Surface-enhanced resonance Raman scattering (SERRS) is shown to be a unique tool to perform selective analytical spectroscopy of a specific layer in a bilayer sample without apparent interference from adjacent material. The spatial spectroscopic tuning was achieved on Langmuir–Blodgett monolayers of two different molecules with electronic absorption in the visible. Since the surface Raman electromagnetic enhancement extends well beyond the first adsorbed monolayer, it is possible for the SERRS of upper layers to be much stronger than the surface-enhanced Raman scattering (SERS) signal from the first monolayer deposited onto a Ag surface. The SERS active surface was of Ag-coated Sn spheres that have been shown to be good enhancing surfaces in a wide spectral region encompassing that of the Ag and Au island films.

The interest in the structure and characterization of Langmuir–Blodgett (LB) monolayer film assemblies continues to grow in view of their wide scope of applications, especially in the field of molecular electronics.[1,2] For monomolecular layers or mixed layers with submonolayer concentrations, molecular sensitive analytical techniques are needed to study, for instance, chemical reactions[3] in LB monolayers and changes due to interactions at the interface. Surface-enhanced Raman spectroscopy[4] and, in particular, SERRS[5,6] provide both molecular specificity and sensitivity for monolayer and submonolayer quantities.[7,8] There are alternative ways in which the sensitivity of the inelastic scattering can be improved to be applied to the study of thin monolayer assemblies, for example, waveguide Raman scattering[9] (WRS) or simply resonant Raman scattering.[10] However, it is shown here that SERRS is a unique nondestructive method for selective vibrational characterization of monolayers and submonolayer film assemblies. By tuning into molecular resonances and plasmon resonances[11] of the enhancing surfaces and using the fact that there exists electromagnetic enhancement at a distance above the surface (up to ca. 10 nm), the spectral properties of specific components in multilayers and/or mixed-layer assemblies could be probed. The feasibility of this spectroscopic tuning is demonstrated here for LB monolayers of two molecular dyes with strong electronic absorption in the visible.

Experimental Section

Langmuir–Blodgett monolayers of (t-Bu)$_4$VOPc and N, octyl-substituted 3,4:9,10-perylenebis(dicarboximide) {Oc-PTCDNH} (see Figure 1) were prepared at room temperature and transferred to Corning 7059

glass slides or slides with Ag-coated Sn spheres in a Lauda trough equipped with an electronically controlled film deposition device. Monolayers were compressed at a speed of 0.1 A^2/molecule/s, and the film transfer was carried out at 4.8 mm/min at a pressure of 10 dynes/cm. Monolayers were transferred by substrate withdrawal (or Z-type deposition). For spreading onto the water surface the (t-Bu)$_4$VOPc and the Oc-NPTCNH were dissolved in toluene. Ag-coated Sn spheres[12] were formed by evaporating 100 nm mass thickness of Sn at a rate of 0.5 nm/s onto glass substrate heated at 120 °C. An amount of 100 nm of Ag was then overlaid with the substrate held at room temperature. The 514.5-, 568.2-, and 647.1-nm lines of the Ar$^+$ and Kr$^+$ ion laser were used with a typical power of 100 mW. Raman shifts were measured with a Spex-1403 and a Ramanor-1000 double monochromator (with micro-

(1) Swalen, J. D. *J. Mol. Electron.* **1986**, *2*, 155–181.
(2) Roberts, G. G. In *Electronic and Photonic Applications of Polymers*; Bowden, J. M., Turner, S. R., Eds.; American Chemical Society: Washington, DC, 1988; p 225.
(3) Bubek, C. *Thin Solid Films* **1988**, *160*, 1–14.
(4) *Surface Enhanced Raman Scattering*; Chang, R. K., Furtak, T. E., Eds.; Plenum: New York, 1982.
(5) Efrima, S. In *Modern Aspects of Electrochemistry*; White, E., Bokris, J. O. M., Conway, B. E., Eds.; Plenum: New York, 1985; Vol. 16, p 253.
(6) Zeman, E. J.; Carron, K. T.; Schatz, G. C.; Van Duyne, R. P. *J. Chem. Phys.* **1987**, *87*, 4189–4200.
(7) Aroca, R.; Jennings, C.; Kovacs, G. J.; Loutfy, R. O.; Vincett, P. S. *J. Phys. Chem.* **1985**, *9*, 4051–4054.
(8) Kim, J. H.; Cotton, T. M.; Uphaus, R. A. *Thin Solid Films* **1988**, *160*, 389–397.
(9) Rabolt, J. F.; Swalen, J. D. *Advances in Infrared and Raman Spectroscopy*; Clark, R. J. H., Hester, R. E., Eds.; John Wiley & Sons: Chichester, 1988; Vol. 16, pp 1–36.
(10) Harrand, M.; Masson, M. *J. Chem. Phys.* **1987**, *87*, 5176–5185.
(11) Moskovits, M. *Rev. Mod. Phys.* **1985**, *57*, 783–826.
(12) Aroca, R.; Kovacs, G. J. *J. Mol. Struct.* **1988**, *174*, 53–58.

* Author to whom correspondence should be directed.